

D34  
N82-13699

MODELING HUMAN TRACKING ERROR IN  
SEVERAL DIFFERENT ANTI-TANK SYSTEMS<sup>†</sup>

David L. Kleinman

ALPHATECH, Inc. and University of Connecticut

SUMMARY

The Optimal Control Model (OCM) of human response serves as a mechanism for generating sample time histories of human tracking error in different anti-tank systems. The systems under study include TOW (Tube-Launched Optically Guided System), DRAGON (Shoulder Mounted) and ITV (Improved TOW Vehicle). The model-generated trajectories are compared with field-test data across several dimensions including time-domain (temporal) statistics, frequency content and subjective comparisons on individual runs.

MODELING APPROACH

The objective of this work is to develop a computerized model for generating human tracking error time histories in several different anti-tank systems. The systems include those in common use by the US Army such as TOW, DRAGON and ITV. A fourth system - GLLD (Ground Launched Laser Designator) is similar to TOW and will not be discussed here. Of these systems, TOW and DRAGON are basically command line-of-sight (LOS), whereas ITV is a rate command system. The model that is developed must produce accurate facsimiles of tracking error over a wide range of target trajectories, from crossing (straight-line) motion to maneuvering motion. The model must be causal in the sense that future target motions are unknown at the present time.

For the systems and target passes considered here, target motion is restricted to the azimuth axis, i.e. the gunner and target vehicle are both at the same ground level. Tracking error in elevation arises solely from the human's inherent motor and observation randomness. Although the model that we have developed treats both axes, we discuss primarily the results for the azimuth axis here. A more complete discussion and presentation of the results may be found in Ref. [1].

The Optimal Control Model

The Optimal Control Model of human response is used as the mechanism for building the anti-tank tracking model. The OCM technology has been successfully applied in numerous contexts including pilot control, anti-aircraft artillery, etc. The mechanics of using the OCM to generate sample path time-histories (as opposed to statistical measures) is described in Ref. [2]. Our application follows this approach, with minor modifications to account for the dual-axis nature of the tracking task. The pertinent

<sup>†</sup>Supported by Army Material Systems Analysis Agency on Contract DAAK11-80-C-0050

equations for Monte-Carlo/Sample Path Simulation using the OCM may be found in Ref. [2].

Application of the OCM requires specification, for each given system-display-manipulator dynamics, of 1) the operator's task objectives in terms of a set of cost functional weights, 2) the parameters that define the operator's inherent limitations, and 3) an "internal" model of the target dynamics. With these items specified optimal control and estimation theory is used to obtain the human's feedback strategy, and generate closed-loop performance results.

1. *Task Objectives:* For a basic tracking task, wherein the human attempts to keep the error  $e(t)$  small, we use a cost functional

$$J(u) = E\{e^2(t) + Q_e \dot{e}^2(t) + Q_u \dot{u}^2(t)\} \quad (1)$$

The weighting  $Q_e$  reflects a human's subjective weighting on error rate. It is indicative of strategy, style or technique and could be associated with the type of training on a given system. The weighting  $Q_u$  on error rate induces a first-order lag that is associated with the neuro-motor system dynamics. For each system we select  $Q_u$  to yield  $\tau_n$  = neuro-motor time-constant = .1 sec. The value of  $Q_e$  is to be determined for each system, based on data comparisons.

2. *Human Operator Limitations:* The primary human operator limitations modeled in the OCM are those associated with perceiving displayed quantities and executing intended control motions. The observational submodel in the OCM assumes that the human observes tracking error  $y_1(t) = e(t)$  and tracking error rate  $y_2(t) = \dot{e}(t)$ . However, the human perceives a delayed and noisy replica of these signals via

$$y_{pi}(t) = F_i[y_i(t - \tau)] + v_{yi}(t - \tau) \quad i = 1, 2 \quad (2)$$

The function  $F(\cdot)$  represents a visual/indifference threshold of value  $a_1 = 0.6$  mr ÷ display gain on error and  $a_2 = .5a_1$  on error rate. The time-delay  $\tau = .15$  sec. Each observation noise is white with covariance

$$v_{yi}(t) = \rho_{yi} E\{y_i^2(t)\} / \text{ATTN} \quad (3)$$

Where  $\rho_{yi} = .01\pi$  (-20dB); the attention allocations are assumed split 0.8 for azimuth vs 0.2 for elevation.<sup>†</sup> The nominal parameter values associated with the observational submodel are assumed fixed for all systems and target types considered.

The neuro-motor submodel for generating human corrective inputs is given by

$$\tau_n \dot{u}(t) + u(t) = u_c(t) + v_u(t)$$

<sup>†</sup> A more precise model would be to employ dynamic attention allocation.

The quantity  $u_c(t)$  is the "commanded" control input that is generated from the Kalman Filter/Predictor/Gains cascade;  $\tau_n$  is the neuro-motor time constant. The white motor-noise  $v_u(t)$  consists of an additive plus a ratioed component for each axis. The covariance of the motor-noise for azimuth and elevation axes, respectively, is

$$V_{uA} = V_{uA}^0 + \rho_{AA} E\{u_{cA}^2(t)\} + \rho_{AE} E\{u_{cE}^2(t)\} \quad (4a)$$

$$V_{uE} = V_{uE}^0 + \rho_{EA} E\{u_{cA}^2(t)\} + \rho_{EE} E\{u_{cE}^2(t)\} \quad (4b)$$

The crossfeeds  $\rho_{AE}$  and  $\rho_{EA}$  model uncertainty/randomness in one axis resulting from manipulator motion in the other axis. For the systems/targets studied, elevation commands  $u_{cE}$  are small relative to azimuth commands  $u_{cA}$  (recall target motion is in azimuth only). Thus,  $\rho_{EE}$  and  $\rho_{AE}$  are not readily obtained from the available data. Therefore, we have assumed

$$\rho_{AA} = \rho_{EE} = \rho_u \quad \text{and} \quad \rho_{AE} = 0 \quad (5)$$

The remaining quantities  $V_{uA}^0$ ,  $V_{uE}^0$ ,  $\rho_u$ ,  $\rho_{EA}$  are system/manipulator dependent. Their values must be elicited from model - data comparisons. Finally, Eq(4) shows that the motor-noise scales with commanded control input  $u_c(t)$ . In some instances, e.g. command LOS systems, it is more natural for motor-induced randomness to scale with commanded rate  $\dot{u}_c(t)$ .

3. *Target Submodel:* In the present application of the OCM to track ground targets, target velocity  $\dot{\theta}_T(t)$  and acceleration  $\ddot{\theta}_T(t)$  are generally small. Thus, we use a simple internal model for target motion

$$\dot{x}(t) = w_d(t) \quad (6)$$

where  $x(t)$  is the human's internal representation of target velocity. The "driving noise"  $w_d(t)$  has covariance

$$\text{cov}[w_d(t)] = \beta \ddot{\theta}_T^2(t) + \alpha \dot{\theta}_T^2(t) \quad (7)$$

Note that the "truth" model is  $\dot{x}(t) = \ddot{\theta}_T(t)$ . The values selected for  $\alpha$  and  $\beta$  are

$$\beta = 10^2, \quad \alpha = .015^2 \quad (8)$$

These values are constant across all systems and targets studied.

#### Data-Model Comparison Procedures

The OCM can be used to generate, for a given system and target trajectory, an ensemble of tracking error time histories  $E_m = \{e_j(t) ; j = 1, \dots, M\}$ . These model-generated runs may be compared against an ensemble of equivalent data trials,  $E_d$ . Clearly, it is the statistics of these two ensembles that one would wish to compare via model-data validation tests. Several modes of comparison are possible, discussed below. For consistency we have found it useful to remove the temporal mean  $\mu_{ej}$  from each run prior to analysis.

Thus,

$$e_j(t_i) = e_j(t_i) - \mu_{ej} ; \mu_{ej} = \frac{1}{N} \sum_{i=1}^N e_j(t_i) \quad (9)$$

where  $t_i, i = 1, \dots, N$  are the sampled values of  $e_j(t)$ . This procedure removes random variations in signal mean, DC bias offsets in field recording equipment, biases in human aiming point, etc.

1. *Ensemble Analysis:* The ensemble mean and standard deviation can be computed in the usual manner,

$$\mu_e(t) = \text{Ensemble mean} = \frac{1}{M} \sum_{j=1}^M e_j(t) \quad (10a)$$

$$\sigma_e(t) = \text{Ensemble SD} = \left\{ \frac{1}{M-1} \sum_{j=1}^M [e_j(t) - \mu_e(t)]^2 \right\}^{1/2} \quad (10b)$$

Since the sample runs have been rendered zero (temporal) mean we would expect  $\mu_e(t) \approx 0$  if the ensemble was stationary.

2. *Temporal Analysis:* If the ensemble  $E$  is stationary,  $\mu_e(t) \approx 0$  and  $\sigma_e(t) \approx \text{constant}$  so that the information content in the temporal ensemble is reduced to a single number, i.e. RMS tracking error. A more direct way to obtain average RMS tracking error is to compute the temporal statistic

$$\sigma_{ej} = \left[ \frac{1}{N-1} \sum_{i=1}^N e_j^2(t_i) \right]^{1/2} \quad (11)$$

for each run, and form the composite, M-run average, via

$$\sigma_e = \frac{1}{M} \sum_{j=1}^M \sigma_{ej} \quad (12)$$

However, unlike the ensemble analysis,  $\sigma_e$  is meaningful only in the stationary case. Its computation in the non-stationary case is possible, but of dubious interpretation.

3. *Frequency Domain Analysis:* The RMS temporal metrics give an indication of total error power, they do not indicate how this power is distributed over the frequency range, whether there exists resonances, etc. To obtain these later indicators of system response we compute, from the temporal ensemble  $E = \{e_j(t), j = 1, \dots, M\}$ , a frequency domain ensemble of normalized error PSD,  $E^* = \{e_j^*(\omega), j = 1, \dots, M\}$  where

$$e_j^*(\omega) = \left| \frac{1}{\sigma_{ej}} \sum_{i=1}^N e_j(t_i) \exp[-j\omega t_i] \right| \quad (13)$$

Normalization greatly reduces the sensitivity to motor-noise and inter-subject variability since it considers only relative power distribution over  $\omega$ . Note that the PSD computations are strictly valid for a sta-

tionary ensemble; their computation is possible for any ensemble, of course, but the interpretation in the non-stationary case is dubious.

The ensemble  $E^*$  of normalized error PSD can be averaged (in the same manner as  $E$ ) via equations similar to (10a - 10b) to yield the ensemble mean  $\mu_e^*(\omega)$  and ensemble SD,  $\sigma_e^*(\omega)$ . Comparison of model and data PSD statistics is thus possible and provides another, interesting, facet for model validation.

## RESULTS

In this section model-data comparisons are given for the three anti-tank systems considered. In each case it is necessary to provide a description of the system-manipulator dynamics, and values for the motor-noise parameters and error rate weighting  $Q_e$ .

### TOW System

The TOW system is a command LOS system consisting of a launch tube plus sight mounted on a viscous (rate) damped turret. Thus the torque supplied by the operator to point the sight varies with sight (i.e. control) rate. The dynamical model used for the TOW system is

$$T(s) = \frac{1}{Ts+1} ; \quad T = 0.1 \text{ sec.} \quad (14)$$

These dynamics are chosen for convenience<sup>†</sup>, and are viewed as representative of the manipulator (arm-viscous mount) characteristics.

In our data-model analysis of the TOW system we found  $Q_e \approx 0$  gave best match. The motor-noise in the OCM is assumed to scale with Commanded (i.e. LOS) rate, and the pertinent noise parameters (obtained from matching RMS scores) are

$$V_u^0 = [.05, .01], \quad \rho_u = .005, \quad \rho_{EA} = .015$$

The temporal RMS statistics, computed via Eqs (11)-(12), for three different ensembles are given in Table 1. The TF and TS ensembles correspond to crossing targets at a range of 3Km with  $\dot{\theta}_T = 5.47$  and  $\dot{\theta}_T = .55$  mr/sec, respectively. These ensembles are stationary. The TM ensemble corresponds to a set of 19 maneuvering trials. In these cases the target was approaching the gunner following a serpentine path with  $\dot{\theta}_T \sim 1$  mr/sec,  $\ddot{\theta}_T \sim .5$  mr/sec<sup>2</sup> peak values. Each target pass was somewhat different; this ensemble is not stationary.

The model-data comparisons shown in Table 1 are excellent for both azimuth and elevation axis tracking (The numbers in parentheses are the computed standard deviations in the RMS tracking errors.) Only the elevation SD is not well-matched for the maneuvering trials. This discrepancy is expected to be corrected by a dynamic attentional submodel. A comparison of

<sup>†</sup> At least first-order dynamics are required by the OCM.

model-data normalized PSD ensemble statistics is shown in Figs. 1-2 for the TF ensemble. The results are in excellent agreement. A t-test performed pointwise was used to confirm the equality of the PSD means at the 95% confidence level.

TABLE 1 - COMPARISON OF TEMPORAL TRACKING ERRORS, TOW SYSTEM

| M     | Azimuth SD   |              | Elevation SD |              |
|-------|--------------|--------------|--------------|--------------|
|       | Data         | Model        | Data         | Model        |
| TF 23 | 0.106(0.017) | 0.119(0.018) | 0.050(0.009) | 0.052(0.009) |
| TS 19 | 0.057(0.005) | 0.054(0.004) | 0.030(0.006) | 0.031(0.005) |
| TM 19 | 0.35 (0.10)  | 0.35 (0.07)  | 0.14 (0.02)  | 0.05 (0.01)  |

Individual runs produced by model and data can also be compared subjectively. Fig 3 is a comparison of a model and a data run from the TF ensemble. Fig 4 likewise is a comparison of model-vs-data trials for one of the maneuvering target passes. The "eyeball" similarity is quite impressive.

#### DRAGON System

The DRAGON is a shoulder-mounted system that consists of a launch tube plus sight. The front of the tube is pivoted on a support; the rear part of the tube rests on the operator's shoulder. Thus, as the operator (usually in a seated position) tracks a crossing target he must continuously move his shoulder by leaning his torso more and more to one side. There are no dynamics associated with the system per-se. The only dynamics are those associated with the operator's torso--i.e. the control "manipulator". These dynamics are approximated as

$$T(s) = \frac{s/\beta + 1}{\left(\frac{s}{\omega_n}\right)^2 + 2\zeta\left(\frac{s}{\omega_n}\right) + 1} \quad (15)$$

where  $\omega_n = 11 \pm 1$  rad/sec,  $\beta = 3 \pm 1$  and  $\zeta = .15$  for tilt in the azimuth axis.

The motor-noise for the DRAGON system is assumed to scale with commanded angle/body tilt as randomness increases greatly if one is required to track while leaning to one side. The motor-noise parameters are

$$V_u^0 = [8, .25], \rho_u = .0001, \rho_{EA} = .000015$$

The weighting on error rate  $Q_e \approx 0$ .

The tracking error data for DRAGON consisted of  $\approx 40$  passes of a crossing target at 1km with  $|\dot{\theta}_T| = 10$  mrad/sec. In approximately 1/2 of the runs the target moved from right to left (DR); in the other runs motion was from left to right (DL). A comparison of the temporal RMS statistics of model-vs-data is shown in Table 2. The results are excellent, but this is not a stationary

ensemble as the motor-noise covariance increases during the course of a run! Indeed, Figs 5-6 show the true nature of the tracking error ensemble for model and data. This is a more meaningful comparison than is temporal RMS error.

TABLE 2 - COMPARISON OF TEMPORAL TRACKING ERRORS, DRAGON SYSTEM

| M     | Azimuth SD |           | Elevation SD |            |
|-------|------------|-----------|--------------|------------|
|       | Data       | Model     | Data         | Model      |
| DR 21 | 7.35(3.3)  | 6.82(0.9) | 2.78(1.5)    | 2.73(0.35) |
| DL 22 | 7.2 (2.6)  | 6.82(0.9) | 2.35(1.4)    | 2.73(0.35) |

Comparisons of normalized error PSD for model and data provides another yardstick for judging the effectiveness of the OCM application. As noted earlier, interpretation of these results must be made cautiously as the ensemble is non-stationary. Nevertheless, we can consider this as the "average frequency content" in the error waveforms. Figs 7-8 contain the model-data frequency comparisons for the azimuth axes. The results are excellent. A final model-data validation test is via the subjective comparison of individual tracking error time histories. Fig 9 shows a typical data run vs. a typical sample path from the OCM.

#### ITV System

In the ITV System a TOW mount is driven through rate command dynamics by the human using a handlebar controller. The system dynamics can be approximated by the transfer function

$$T(s) = \frac{K}{s(Ts + 1)} \quad T = \frac{1}{\pi} \text{ sec}, \quad K = .1$$

Since the handlebar is spring-loaded we assume that the motor-noise scales with commanded control input. The motor-noise parameters pertinent to ITV are

$$V_u^0 = [.04, .01], \quad \rho_u = .03, \quad \rho_{EA} = .012$$

In addition, it was found that a weighing  $Q_e \approx .5$  resulted in a best match between model and data PSD ensembles.

TABLE 3 - COMPARISON OF TEMPORAL TRACKING ERRORS, ITV SYSTEM

| M     | Azimuth SD   |              | Elevation SD |              |
|-------|--------------|--------------|--------------|--------------|
|       | Data         | Model        | Data         | Model        |
| 1C 2E | 0.112(0.035) | 0.114(0.027) | 0.092(0.023) | 0.091(0.017) |

There was data from only one ensemble for ITV, corresponding to a crossing target at 2Km with  $\dot{\theta}_T \sim 1$ . The target was moving towards the gunner on a  $40^\circ$  angle. Table 3 gives the model-data comparisons for RMS tracking error in this stationary ensemble. A subjective comparison of a typical model-vs-data time history is given in Fig 10. The comparison of PSD ensemble statistic of model and data is provided in Figs 11-12. Again, we find excellent agreement between OCM results and the field-test data. Note that this agreement is excellent not only for the PSD mean statistics, but also for the 2nd-order statistics that give an indication of the run-to-run variability.

### CONCLUSIONS

It has been demonstrated that the Optimal Control Model can be used to generate accurate facsimiles of target tracking error in various different anti-tank systems. While these results were not entirely unexpected, based on previous applications of the OCM, they are quite interesting in that comparisons have been made across several dimensions. By using the model to generate an ensemble, data and model ensembles can be studied, averaged and manipulated in similar manners, yielding similar results (at least to 2nd order statistics).

The types of systems studied were quite varied, especially with regard to their manipulator characteristics. Thus, it was necessary to adjust the motor-noise parameters in the OCM among systems.

Further application of the OCM to anti-tank tracking systems is expected to refine these results, focus on dynamic inter-axis attentional allocation, and refine techniques for parameter value identification.

### ACKNOWLEDGEMENT

The author would like to acknowledge the personnel at the Army Material Systems Analysis Agency (AMSAA), in particular, Mr. Patrick O'Neil and Mr. Patrick Corcoran, for their support and assistance in supplying what seemed like endless numbers of tracking runs for the various systems studied.

### REFERENCES

1. Kleinman, D.L., "A Model for Generating Human Tracking Error in Anti-tank Systems", ALPHATECH, Inc., Burlington, Mass. Interim Report on Contract DAAK11-80-C-0050, July 1981.
2. Kleinman, D.L., "Monte-Carlo Simulation of Human Operator Response", Technical Report TR77-1. Dept. of EECS, University of Connecticut, 1977.

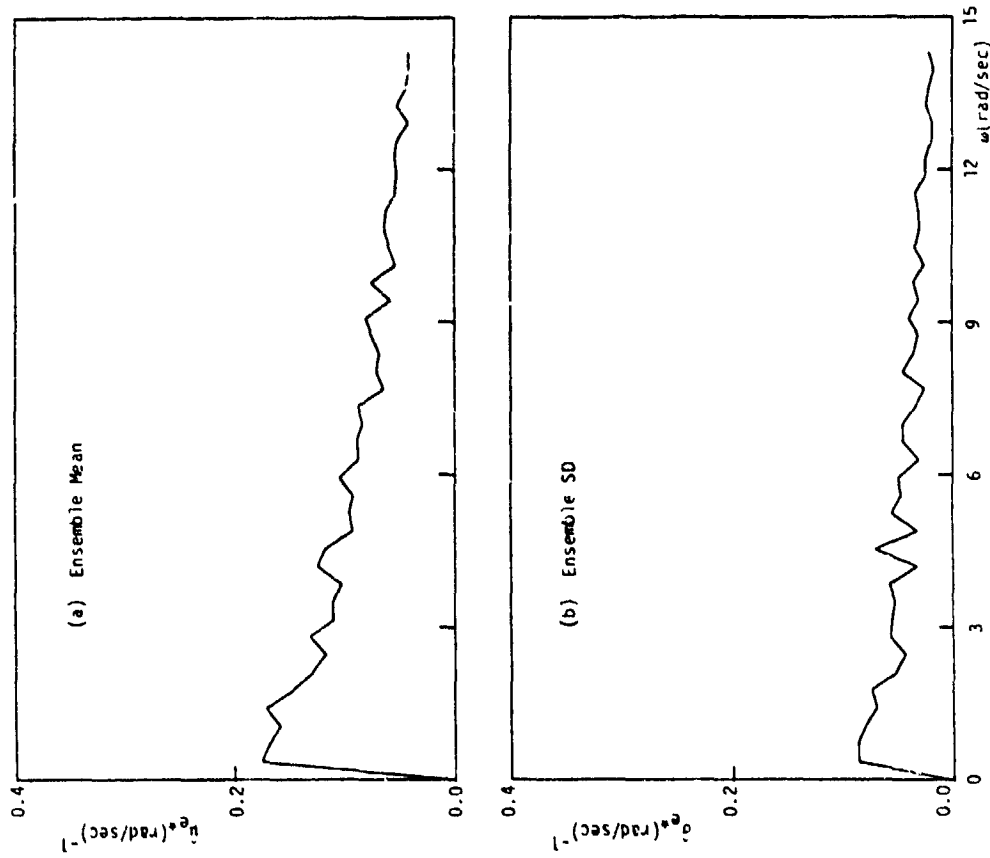


FIGURE 1 - . . . NORMALIZED AZIMUTH ERROR PSD MEASUREMENTS, TOM  
CROSSING TARGET,  $\dot{\theta}_T = 5.47$  MR/SEC,  $N=23$

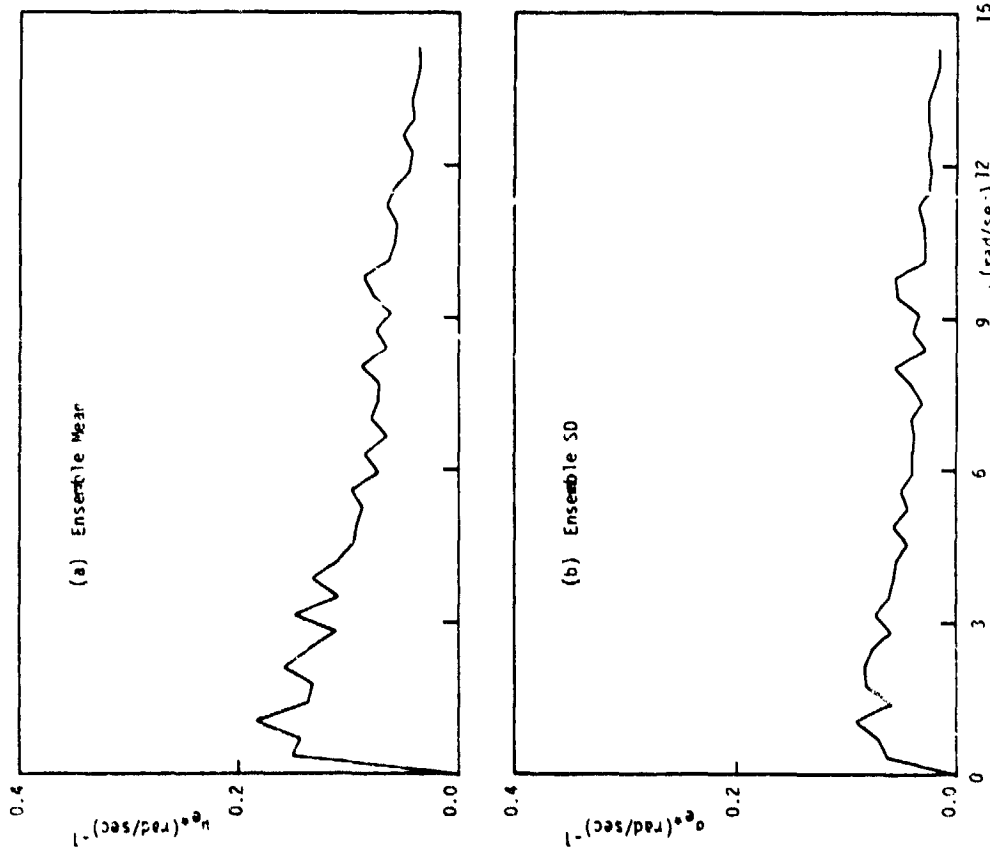


FIGURE 2 - . . . MODELED AZIMUTH ERROR PSD (NORMALIZED), TOM  
CROSSING TARGET,  $\dot{\theta}_T = 5.47$  MR/SEC,  $N=23$

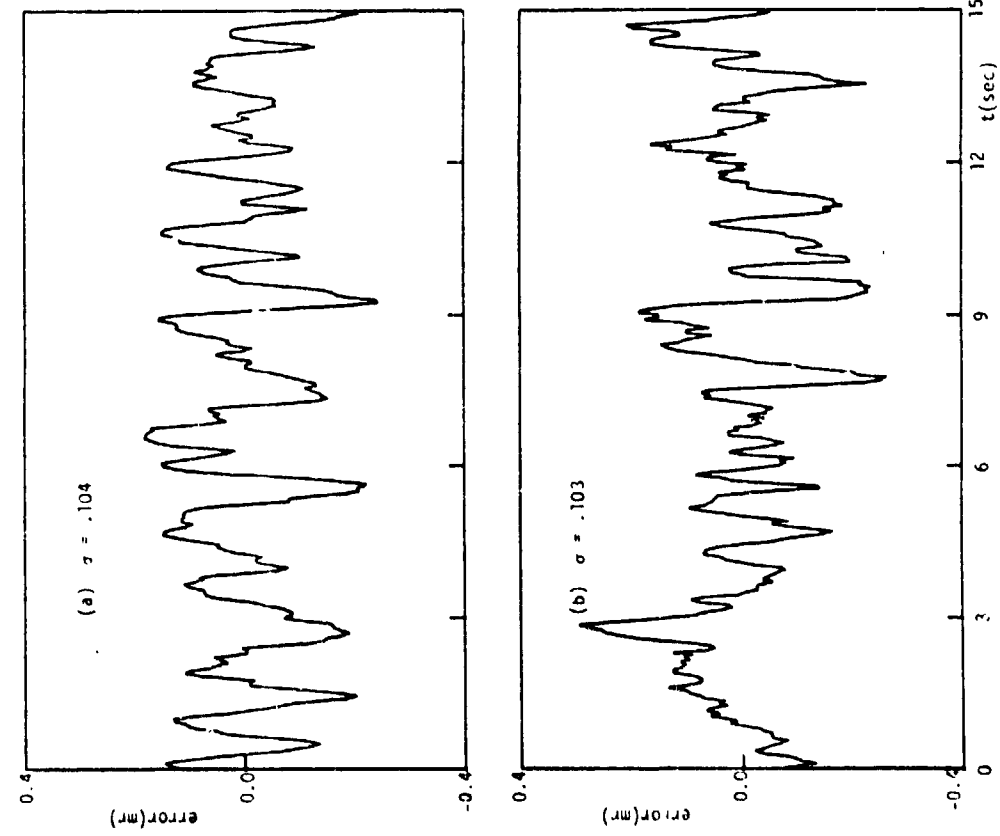


FIGURE 3- . TOW SAMPLE PATHS, AZIMUTH : (A) MODEL, (B) DATA  
CROSSING TARGET,  $\theta_T = 5.47$  MR/SEC

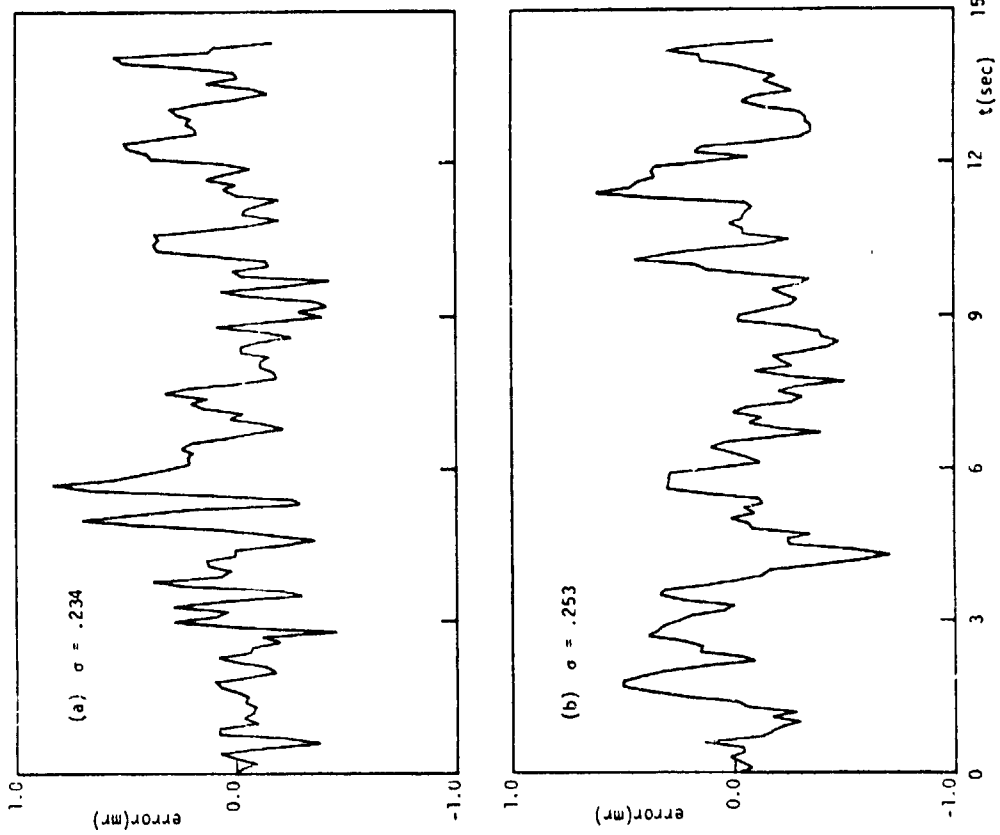


FIGURE 4- . TOW SAMPLE PATHS, AZIMUTH: (A) MODEL, (B) DATA  
MANEUVERING TARGET, TM12

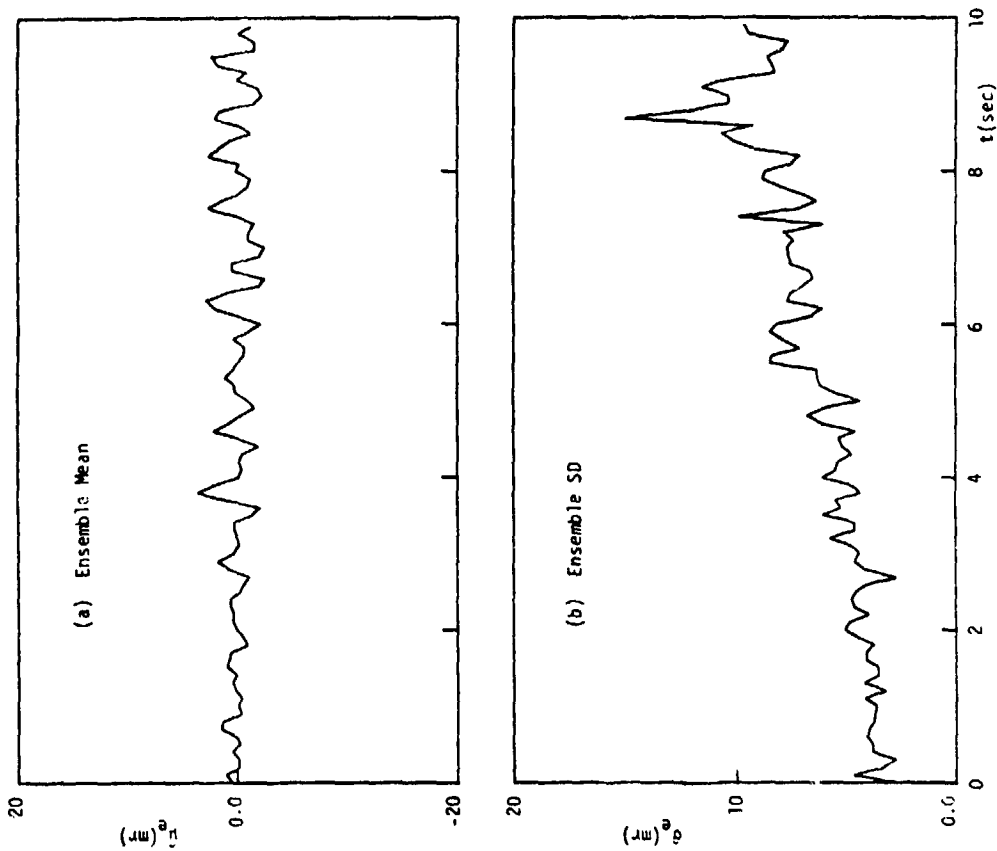


FIGURE 5- . AZIMUTH TRACKING ERROR TEMPORAL DATA, DRAGON CROSSING TARGET,  $\dot{\theta}_T = +10$  MR/SEC (R-L) M=21

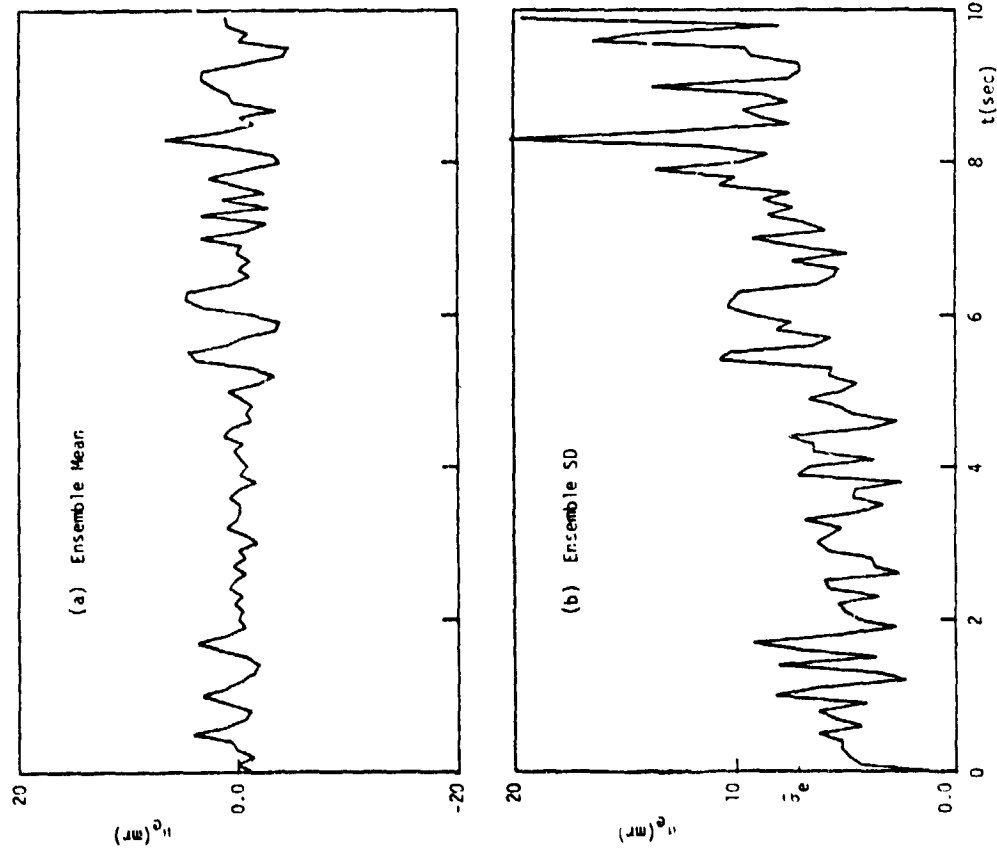


FIGURE 6- . MODELED AZIMUTH TRACKING ERROR STATISTICS, DRAGON CROSSING TARGET,  $\dot{\theta}_T = +10$  MR/SEC, M=21

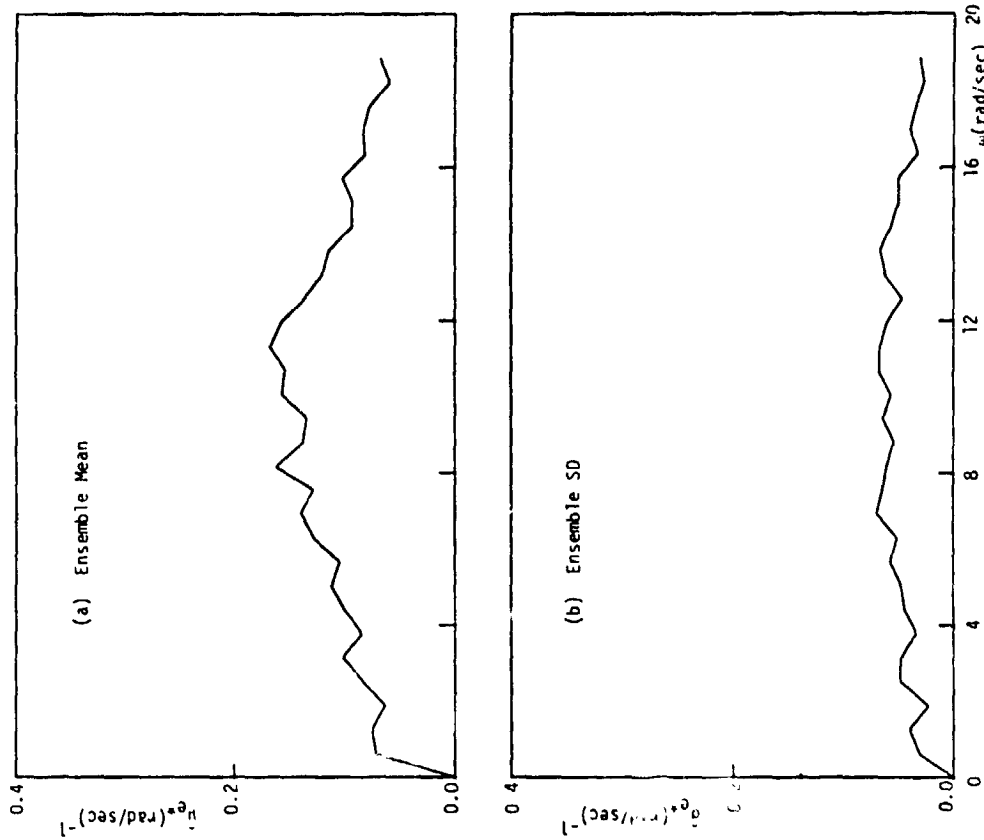


FIGURE 7 - NORMALIZED AZIMUTH ERROR PSD MEASUREMENTS, DRAGON CROSSING TARGET,  $\theta_T = +10$  MR/SEC,  $M=21$

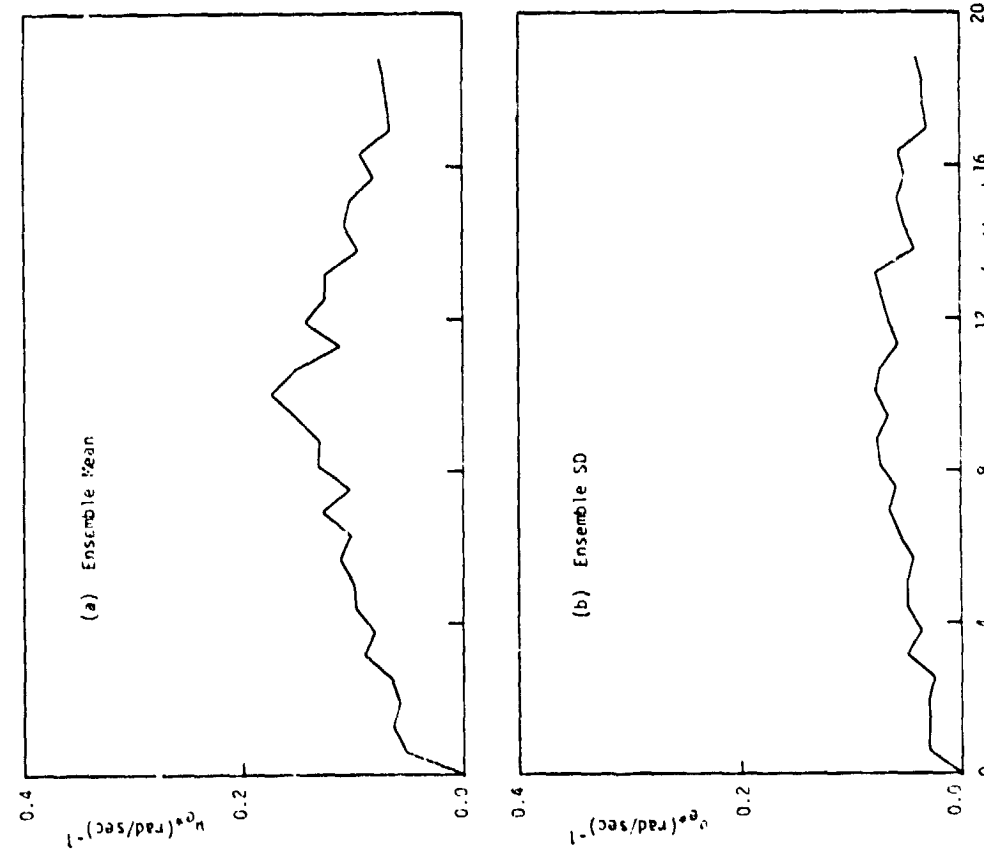


FIGURE 8 - MODELED AZIMUTH ERROR PSD (NORMALIZED), DRAGON CROSSING TARGET,  $\theta_T = +10$  MR/SEC,  $M=21$

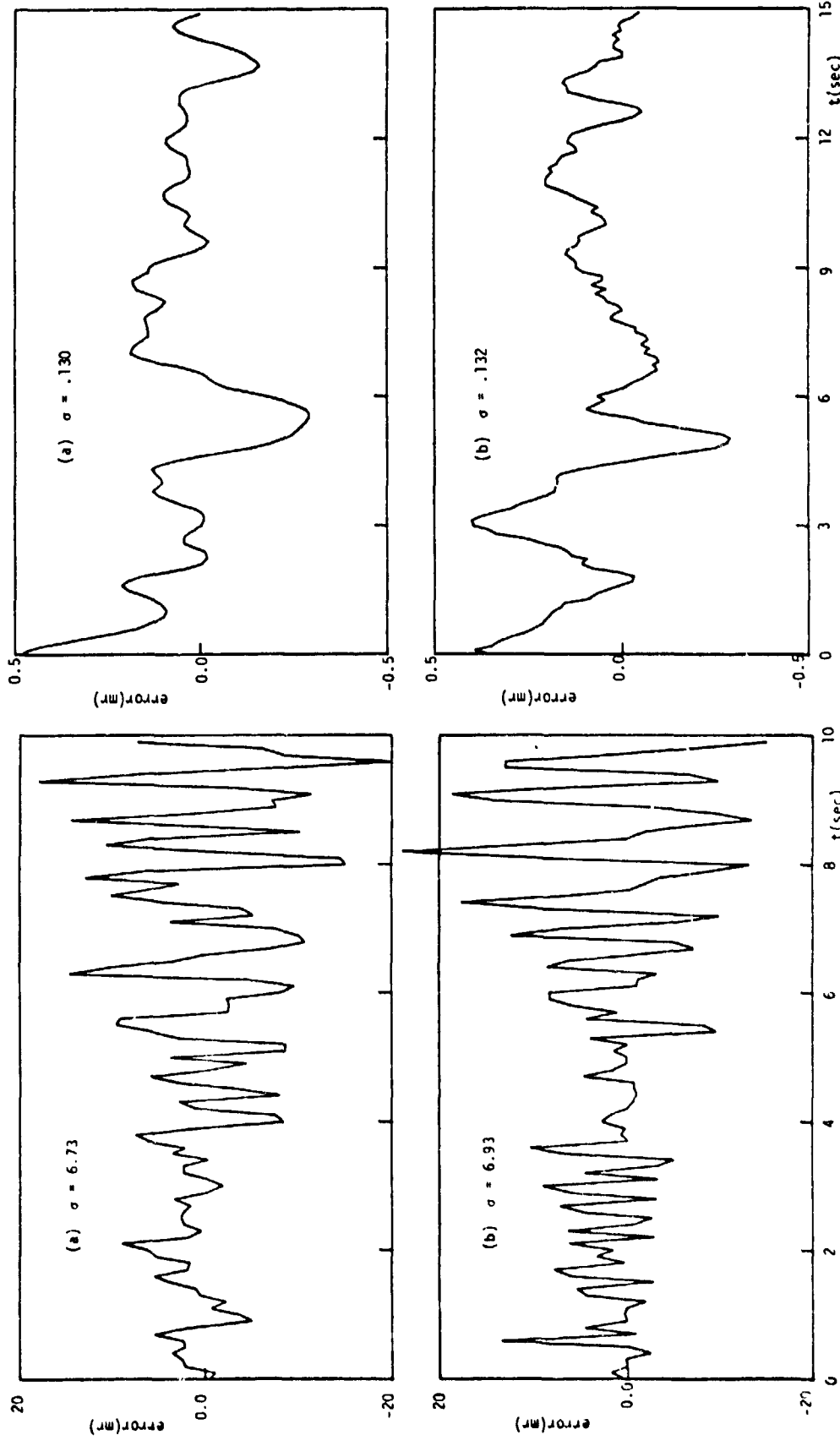


FIGURE 9- . DRAGON SAMPLE PATHS, AZIMUTH : (A) MODEL, (B) DATA  
 CROSSING TARGET,  $\theta_T = +10$  MR/SEC

FIGURE 10- . ITV SAMPLE PATHS, AZIMUTH : (A) MODEL, (B) DATA  
 CROSSING TARGETS,  $\theta_T = 1.0$  MR/SEC

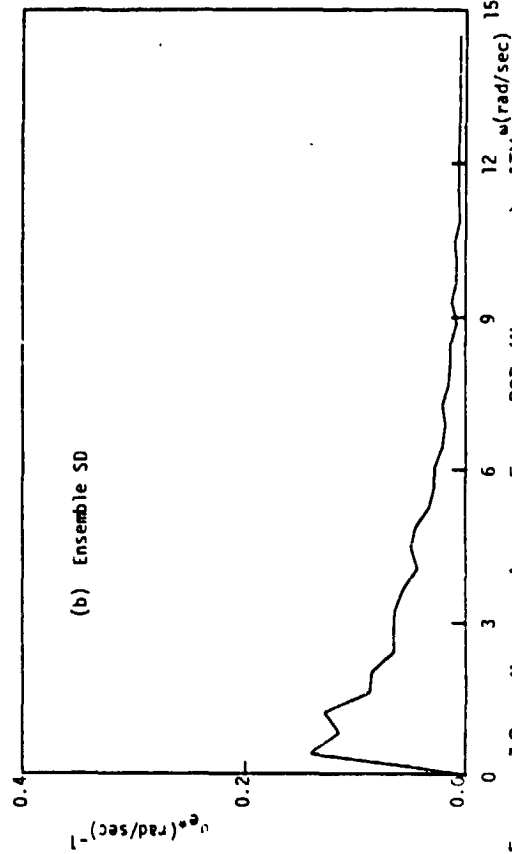
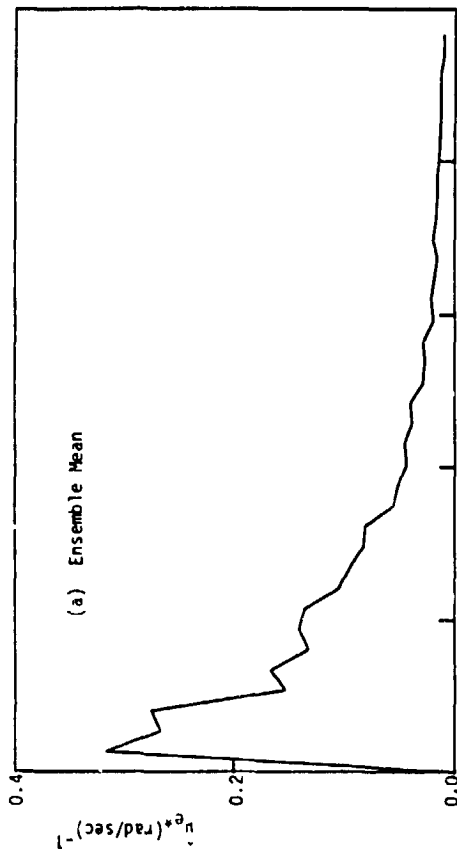


FIGURE 11-. NORMALIZED AZIMUTH ERROR PSD MEASUREMENTS, ITV  
CROSSING TARGET,  $\dot{\theta}_T = 1.0$  MR/SEC,  $M=28$

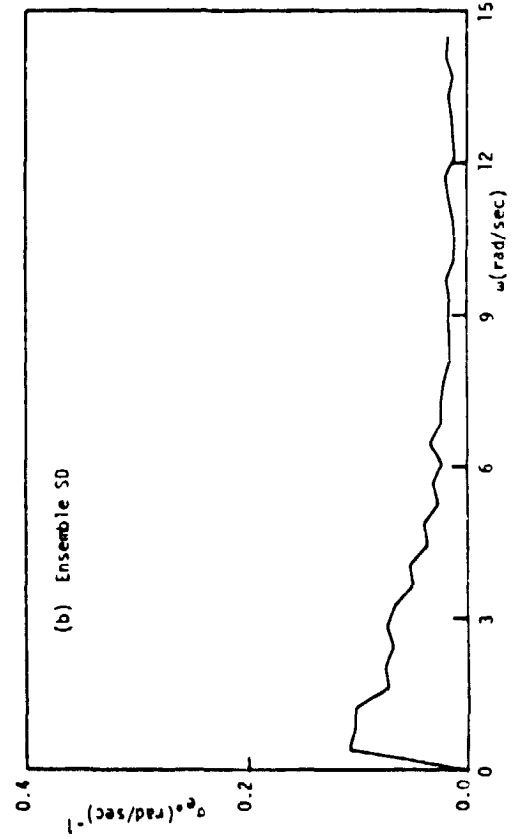
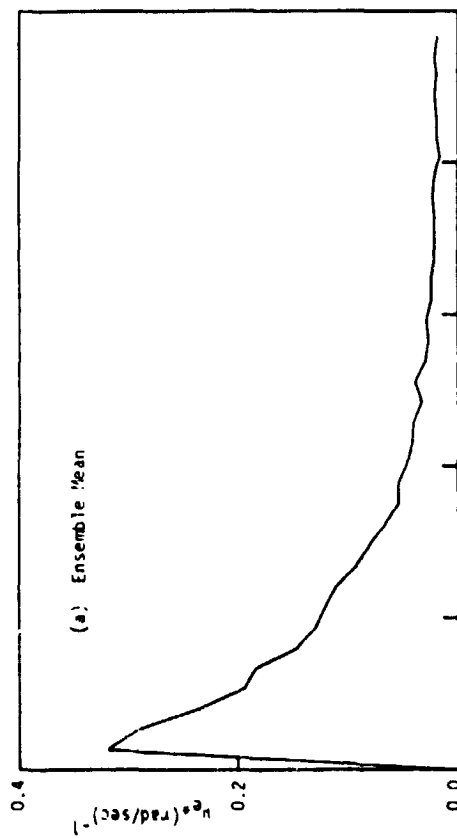


FIGURE 12-. MODELED AZIMUTH ERROR PSD (NORMALIZED), ITV  
CROSSING TARGET,  $\dot{\theta}_T = 1.0$  MR/SEC,  $M=28$